Imaging of the Globe
Anatomy and Pathology

Yi Liang Tan, MBBS, FRCR[a,*],
James Thomas Patrick Decourcy Hallinan, MBChB (Hons) (Bristol), FRCR (UK)[a,b]

KEYWORDS

• Eye globe • CT • MR imaging • Ocular inflammatory disorder • Intraocular tumors
• Postoperative imaging

KEY POINTS

- Since the advent of computed and MR imaging, ophthalmic imaging has significantly advanced, allowing for detailed evaluation of the eye globe allowing even detection of subtle globe abnormalities on dedicated and non-dedicated studies.
- This article aims to highlight the relevant anatomy of the globe and illustrate the imaging features of common ocular conditions.
- This article covers commonly encountered clinical conditions; congenital and acquired ocular abnormalities, ocular detachments, inflammatory disorders, trauma, incidental ocular calcifications, and post-surgical changes with illustrative imaging examples.

INTRODUCTION

Advances in computed tomography (CT) and MR imaging (MRI) have significantly enhanced the visualization and detection of ocular abnormalities. With improved spatial resolution, assessment of the globes and orbits now requires a more structured and systematic diagnostic approach. In order to interpret the globe abnormality, a proficient understanding of the globe anatomy is essential. Knowledge of the imaging features of both traumatic and non-traumatic globe abnormalities is necessary to ensure accurate diagnosis and appropriate ophthalmology referral. In addition, recognizing incidental findings such as degenerative changes, globe implants, and fillers are important to prevent unnecessary investigations. This article highlights common pathologic processes affecting the various anatomic layers of the globe, illustrated through case examples, and aims to familiarize readers with the imaging features of frequently encountered ocular diseases.

GLOBE ANATOMY

The globe occupies about one-third of the bony orbit. Its wall has 3 concentric layers: an outer fibrous coat (sclera and cornea), a vascular uvea (choroid, ciliary body, and iris), and an inner neural retina; the whole globe is invested by Tenon's fascial capsule. The lens divides the globe into an anterior segment, filled with aqueous humor and accounting for roughly one-sixth of globe volume, and a posterior segment, filled with vitreous humor, which constitutes the remaining five-sixths.[1]

Tenon's Capsule

The outermost fibrous layer of the eye comprises the sclera and the cornea. The sclera is enveloped in Tenon's capsule, a thin fascial sheath that separates the globe from orbital fat and creates a socket-like enclosure. Anteriorly the capsule merges with the bulbar conjunctiva, and posteriorly it fuses with the optic nerve sheath. The optic

[a] Department of Diagnostic Imaging, National University Hospital, 5 Lower Kent Ridge Road, 119074, Singapore; [b] Department of Diagnostic Radiology, Yong Loo Lin School of Medicine, National University of Singapore, 10 Medical Drive, 117597, Singapore
* Corresponding author.
E-mail address: yi_liang_tan@nuhs.edu.sg

Radiol Clin N Am 64 (2026) 659–673
https://doi.org/10.1016/j.rcl.2025.09.002
0033-8389/26/© 2025 Elsevier Inc. All rights are reserved, including those for text and data mining, AI training, and similar technologies.

Descargado para Lucia Angulo (lu.maru26@gmail.com) en National Library of Health and Social Security de ClinicalKey.es por Elsevier en julio 20, 2026.
Para uso personal exclusivamente. No se permiten otros usos sin autorización. Copyright ©2026. Elsevier Inc. Todos los derechos reservados.

Abbreviations

CT	computed tomography
MR	magnetic resonance
GDD	glaucoma drainage device
PFV	persistent fetal vasculature
ROP	Retinopathy of prematurity
RPE	retinal pigment epithelium

nerve, its sheath, and the ciliary nerves and vessels perforate the capsule posteriorly.[1,2] Tendons of all extraocular muscles pass through the capsule to insert on the sclera, and the capsule reflects along each tendon to form a tubular sheath around the muscle.[2] The capsule's inner surface is smooth and shiny and is separated from the outer sclera by the episcleral or Tenon's space, a potential interval that can extend between fascia and sclera.[3]

Cornea and Sclera

The cornea and sclera together form the tough, outer fibrous layer of the eye, providing protection and structural support for the intraocular contents. The cornea functions as a transparent window that permits the passage of light, and transitions into the sclera at the limbus. The opaque sclera forms the external coat of the globe, which extends posteriorly from the limbus to the optic nerve sheath.[1,3] On MR imaging, the cornea is a low signal intensity structure due to collagen but may be highlighted by an overlying slightly hyperintense tear film on T1-weighted images. The sclera is also composed of collagen, appearing hypointense on MR imaging (**Fig. 1**).

Uvea Tract

The uveal tract is the middle vascular layer of the eye and includes the iris, the ciliary body, and the choroid. These 3 parts are continuous, forming an unbroken coat that has an anterior opening, the pupil, and a posterior gap at the optic nerve canal where the choroid is absent.[4]

The iris is a pigmented, circular diaphragm that controls pupil size and the amount of incoming light. It attaches to the ciliary body, a triangular structure with an anterior ridged pars plicata and a posterior pars plana. The aqueous producing pars plicata contains the ciliary processes, which provide attachment for the zonular fibers of the lens. The pars plana extends posteriorly from the ciliary processes to the ora serrata, the anterior boundary of the retina.[4]

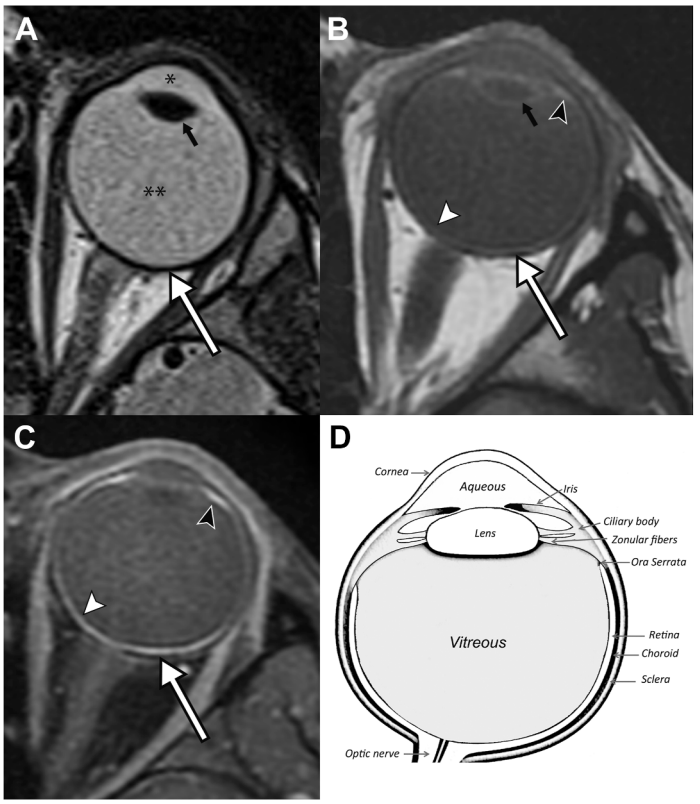

Fig. 1. Normal globe anatomy on MR imaging of the orbits. (*A*) Axial T2-weighted, (*B*) T1-weighted, and (*C*) T1-weighted fat-suppressed contrast-enhanced MR imaging of the orbits. The anterior chamber aqueous humor (*asterisk*) and vitreous humor (*double asterisk*) are diffusely hyperintense on T2-weighted images. The lens (*black arrow*), cornea, and sclera (*white arrow*) appear hypointense on all sequences. The choroid (*white arrowhead*) and ciliary body (*black arrowhead*) show T1-weighted hyperintensity with thin uniform enhancement. (*D*) Simplified annotated illustration of the globe.

Descargado para Lucia Angulo (lu.maru26@gmail.com) en National Library of Health and Social Security de ClinicalKey.es por Elsevier en julio 20, 2026. Para uso personal exclusivamente. No se permiten otros usos sin autorización. Copyright ©2026. Elsevier Inc. Todos los derechos reservados.

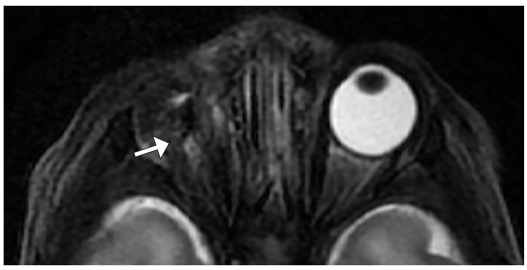

Fig. 2. Axial T2-weighted fat-suppressed sequence demonstrates right anophthalmia with no discernible ocular tissue and a dysplastic optic nerve (*white arrow*).

The choroid forms the posterior part of the uvea, lying between the sclera and the retina. This highly vascular membrane runs from the optic nerve to the ora serrata and is firmly bound to the sclera near the optic nerve and at the sites where the vortex veins exit the eye,[1] which drain into the ophthalmic veins.[4] On MR imaging the uveal tract appears hyperintense on T1-weighted images and hypointense on T2-weighted images (see **Fig. 1**).

Retina

The retina is the innermost sensory layer of the globe and is composed of 2 layers: the outer retinal pigment epithelium (RPE),[4] which is firmly attached to the underlying choroid, and the inner neurosensory retina responsible for visual perception. The sensory retina extends from the optic nerve head to the ora serrata, where it terminates and forms a crenated wavy ring.[3] At this junction, the RPE becomes continuous with the pigmented and non-pigmented layers of the ciliary body and its processes. The retina is firmly adherent only at the margins of the optic nerve head and at the ora serrata.[4] On MR imaging, the retina is in close apposition to the choroid in normal circumstances and cannot be discerned separately.

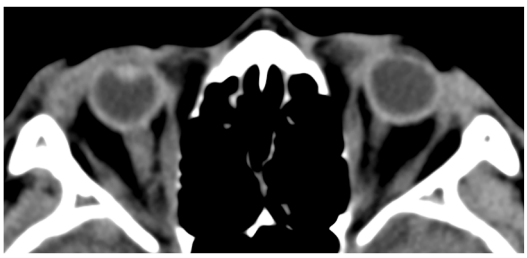

Fig. 3. Unenhanced CT orbits demonstrates small volume globes which appear otherwise normal in configuration, consistent with microphthalmia.

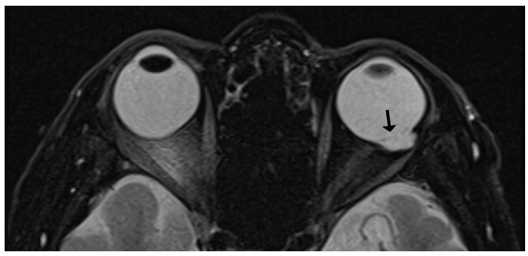

Fig. 4. Axial T2-weighted fat-suppressed sequence showing left micropthalmia with a focal defect at the left posterior globe with associated vitreous humor herniation and retrobulbar cyst (*black arrow*).

Lens

Anterior to the lens lie the iris and the aqueous humor, while posteriorly it is bordered by the vitreous humor. The zonular fibers attach to the outer surface of the equatorial region of the lens capsule and extend outward to the ciliary body, anchoring the lens in place.[1,4]

The space in front of the lens and zonules is divided into 2 chambers by the iris: the larger anterior chamber and the smaller posterior chamber.[4] These chambers are in direct communication through the pupil. On CT, the lens is hyperdense, while on MR imaging it shows hypointensity on both T1-weighted and T2W-weighted images (see **Fig. 1**).

GLOBE PATHOLOGY

Disorders in the Size and Shape of the Globe

Anophthalmia and microphthalmia

Anophthalmia and microphthalmia are rare congenital eye abnormalities. There is usually a small eye or a dysplastic remnant and complete anophthalmia is extremely rare[5] (**Fig. 2**). Microphthalmia is commonly unilateral, but can be bilateral in syndromic cases (**Fig. 3**).

During development, failure in the formation of the optic vesicle or regression of ocular structures already formed may cause microphthalmia or

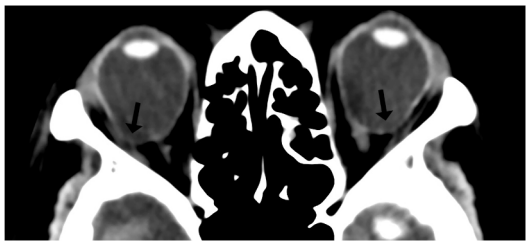

Fig. 5. Unenhanced CT orbits in a patient with myopia showing bilateral posterior staphylomas with elongated globes, focal ectatic appearance of the posterior globe with no scleral defect (*black arrows*).

Descargado para Lucia Angulo (lu.maru26@gmail.com) en National Library of Health and Social Security de ClinicalKey.es por Elsevier en julio 20, 2026.
Para uso personal exclusivamente. No se permiten otros usos sin autorización. Copyright ©2026. Elsevier Inc. Todos los derechos reservados.

Table 1
Types of intraocular detachments, their corresponding potential spaces and involved ocular layers

Type of Detachment	Potential Space	Layers Involved
Posterior hyaloid detachment	Posterior hyaloid space	Fluid between the body of the vitreous and the neurosensory retina
Retinal detachment	Subretinal space	Fluid between the sensory retina and the RPE
Choroidal detachment	Suprachoroidal space	Fluid between the choroid and the sclera

anophthalmia. These may occur in isolation or be associated with ocular disorders including persistent fetal vasculature (PFV), retinopathy of prematurity (ROP), syndromes (eg, fetal alcohol syndrome, and CHARGE syndrome),[6] and congenital infections (e., rubella, toxoplasmosis, varicella, cytomegalovirus).[6] There can also be failure of optic fissure closure, which prevents normal intraocular pressure and produces colobomatous microphthalmia.

Coloboma

Coloboma is a congenital defect that arises when the embryonic optic fissure fails to close, leaving a tissue gap that may involve the iris, lens, retina, choroid, sclera, or optic nerve. Unlike a staphyloma, it reflects tissue loss rather than thinning. The defect usually appears at the fissure site along the inferior globe, and imaging can show a posterior gap with vitreous herniation or a retrobulbar cyst (**Fig. 4**).[7]

Staphyloma

Staphyloma is an outpouching of the wall of the globe, caused by thinning and ectasia of the scleral–uveal coats (**Fig. 5**). All layers of the globe are present but thinned, distinguishing it from coloboma.[8]

INTRAOCULAR POTENTIAL SPACES AND OCULAR DETACHMENTS

Intraocular Potential Spaces

The eye contains several potential spaces where fluid can accumulate, leading to detachment of ocular layers.[1] **Table 1** lists the types of intraocular detachments and potential spaces.[3]

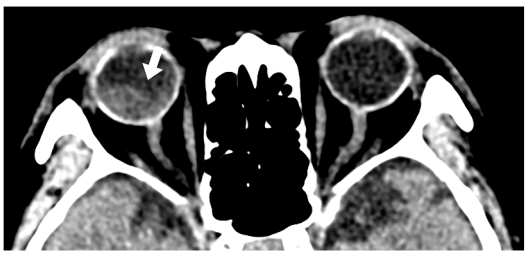

Fig. 6. Unenhanced CT brain with hyperdense fluid along the posterior right globe which crosses the optic disc without attachment, compatible with a posterior hyaloid detachment (*white arrow*).

Posterior Vitreous Detachment

Posterior vitreous detachment is an age-related process in which the posterior vitreous separates from the retina as the vitreous gel degenerates and liquefies. Weakened adhesions allows liquefied vitreous to dissect between the posterior hyaloid membrane and the retina. When detachment is incomplete, residual focal adhesions, often near the optic disc, can mimic retinal detachment on imaging (**Fig. 6**).[9] Traction from the partially

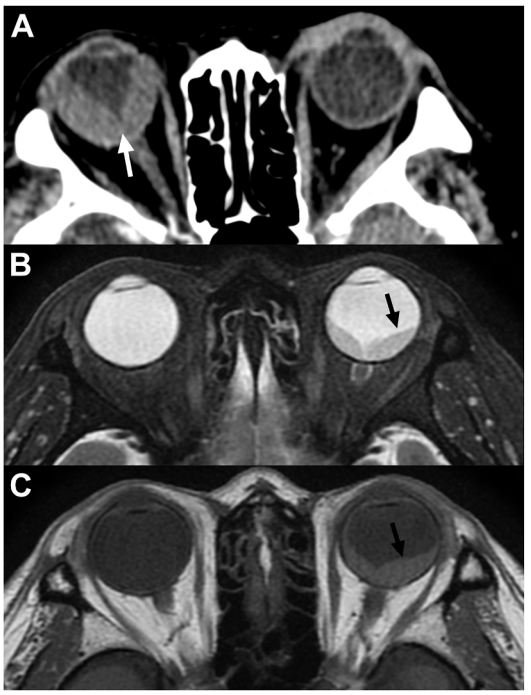

Fig. 7. (*A*) Unenhanced CT showing a right retinal detachment and V-shaped hyperdense subretinal fluid (*white arrow*) extending from the ora serrata to optic disc. (*B*) Axial T2-weighted fat-suppressed and (*C*) axial T1-weighted MR sequences in another patient demonstrates a left retinal detachment (*black arrows*) with T2-weighted and T1-weighted hyperintense subretinal fluid.

Descargado para Lucia Angulo (lu.maru26@gmail.com) en National Library of Health and Social Security de ClinicalKey.es por Elsevier en julio 20, 2026. Para uso personal exclusivamente. No se permiten otros usos sin autorización. Copyright ©2026. Elsevier Inc. Todos los derechos reservados.

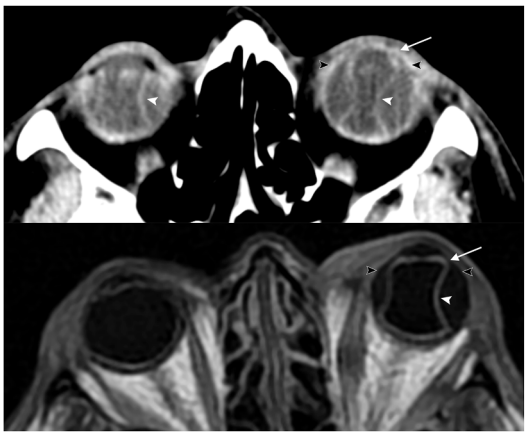

Fig. 8. Contrast-enhanced CT orbits (*top*) and axial T2 fluid attenuated inversion recovery (FLAIR) MR sequence (*bottom*) in 2 patients show characteristic biconvex choroidal detachments, bilateral on CT, and in the left globe on MR (*white arrowheads*). The detachments extend to the ciliary body (*white arrows*) beyond the expected location of the ora serrata (*black arrowheads*).

detached vitreous may produce retinal tears, and vitreous fluid entering a tear can then create retinal detachment.[9]

Retinal Detachment

Retinal detachment is the separation of the sensory retina from the underlying RPE. It is classified as either rhegmatogenous or non-rhegmatogenous.[10] Rhegmatogenous detachment involves a retinal tear that allows fluid to pass into the subretinal space and is most commonly seen in adults, often resulting from vitreous degeneration and

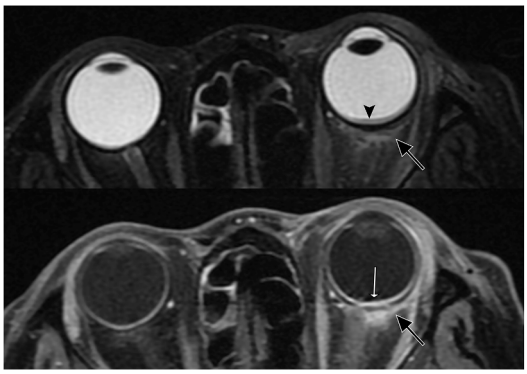

Fig. 9. Axial T2-weighted fat-suppressed (*top*) and fat-suppressed gadolinium-enhanced T1-weighted (*bottom*) MR sequences demonstrate left posterior scleritis with focal scleral enhancing thickening (*white arrow*), episcleral edema and enhancement (*black arrow*). Associated reactive thin subretinal fluid is also seen (*black arrowhead*).

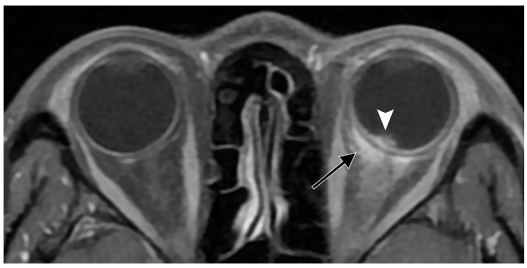

Fig. 10. Axial fat-suppressed gadolinium-enhanced T1-weighted MR sequence demonstrating left posterior scleritis (*black arrow*). This is nodular in appearance and can mimic a choroidal tumor (*arrowhead*). Follow-up imaging showed post-treatment resolution.

traction. Non-rhegmatogenous detachment results from accumulation of fluid beneath the sensory retina without a tear. This implies a breakdown of the blood–retina barrier and may be associated with underlying tumors, infections, inflammatory conditions (eg, posterior scleritis), or vasculopathy.[3] Trauma can lead to retinal detachment with subretinal hemorrhage, which may occur with or without a retinal tear.

On CT and MR imaging, retinal detachment is limited anteriorly by the ora serrata and posteriorly by the margins of the optic disc,[3] resulting in a characteristic V-shaped configuration (**Fig. 7**).[10]

Choroidal Detachment and Choroidal Effusion

Choroidal detachment is the separation of the choroid from the sclera due to accumulation of fluid or blood in the suprachoroidal space. Serous choroidal detachment is primarily caused by ocular hypotony, which increases choriocapillaris permeability and leads to fluid transudation into the suprachoroidal space. It commonly follows intraocular surgery, penetrating trauma, or inflammatory choroidal conditions.[11] Hemorrhagic choroidal detachment is typically associated with

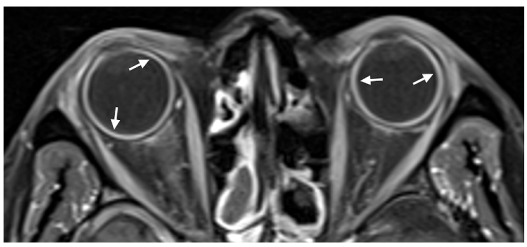

Fig. 11. Axial fat-suppressed gadolinium-enhanced T1-weighted MR sequences of a 52 year old woman with bilateral panuveitis and a history of Behcet's disease. There is diffusely thickened uvea with marked enhancement bilaterally (*white arrows*).

Descargado para Lucia Angulo (lu.maru26@gmail.com) en National Library of Health and Social Security de ClinicalKey.es por Elsevier en julio 20, 2026.
Para uso personal exclusivamente. No se permiten otros usos sin autorización. Copyright ©2026. Elsevier Inc. Todos los derechos reservados.

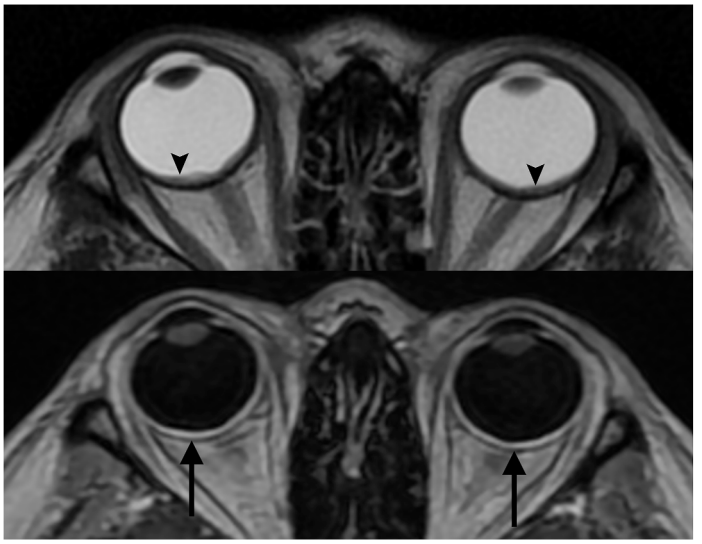

Fig. 12. Axial T2-weighted (*top*) and gadolinium-enhanced T1-weighted (*bottom*) MR sequences of the orbits demonstrating uveitis with bilateral uveal thickening and enhancement (*black arrows*) and subretinal fluid (*black arrowheads*) in a known case of Vogt-Koyanagi-Harada (VKH) disease.

blunt or penetrating ocular injuries or may occur as a complication of intraocular surgery.

On CT and MR imaging, choroidal detachment is often seen as a lenticular collection that can extend anteriorly to the ciliary body and is not limited by the ora serrata. Posteriorly, the choroidal detachments are limited by the vortex vein insertions[3] leading to a classic biconvex morphology (**Fig. 8**).[11]

OCULAR INFLAMMATORY DISORDERS

Scleritis is inflammation of the sclera and the episcleral vascular plexus. It is usually non-infectious and either idiopathic or associated with systemic autoimmune diseases, most commonly rheumatoid arthritis or granulomatosis with polyangiitis.[3,12] Infectious scleritis is rare and typically occurs post-surgery or trauma.[13] Anatomically the condition is anterior or posterior according to its relation to the extraocular muscle insertions.[14] Anterior scleritis presents with pain and visible scleral erythema, whereas posterior scleritis causes pain without erythema. Each form may be diffuse, nodular, or necrotizing.[1]

Imaging is seldom required for anterior scleritis, as the diagnosis is clinical. When CT or MR imaging is performed, it can show scleral enhancement, scleral thickening, and focal periscleral cellulitis (**Fig. 9**). Enhancement may be diffuse, peripheral, or may track along the optic nerve sheath, suggesting optic perineuritis. Nodular scleritis can mimic tumors (**Fig. 10**).[15]

Uveitis is inflammation of the uveal tract, including the iris, the ciliary body and the choroid. It may be idiopathic or linked to systemic disease, often HLA-B27 seronegative spondyloarthropathies or rheumatoid arthritis (**Fig. 11**).[15] Diagnosis rests on radiologic findings, laboratory data and evidence of extra-ocular involvement.[16] Imaging

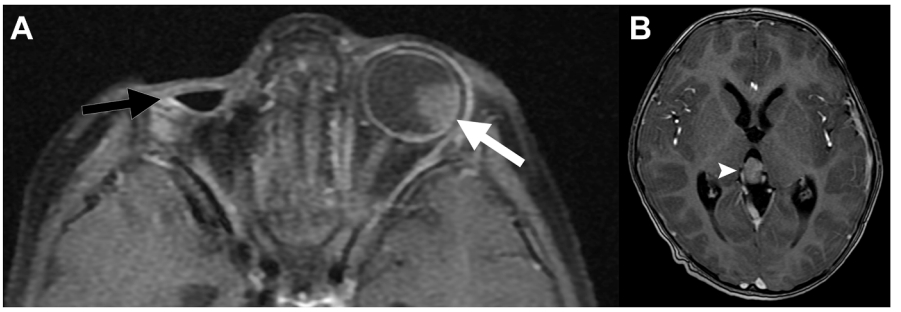

Fig. 13. Axial fat-suppressed gadolinium-enhanced T1-weighted MR sequences of the orbit (*A*) and brain (*B*) demonstrating trilateral retinoblastoma: an enhancing left globe tumor (*white arrow*), right enucleation due to retinoblastoma (*black arrow*) and an enhancing pineal mass (*white arrowhead*).

Descargado para Lucia Angulo (lu.maru26@gmail.com) en National Library of Health and Social Security de ClinicalKey.es por Elsevier en julio 20, 2026. Para uso personal exclusivamente. No se permiten otros usos sin autorización. Copyright ©2026. Elsevier Inc. Todos los derechos reservados.

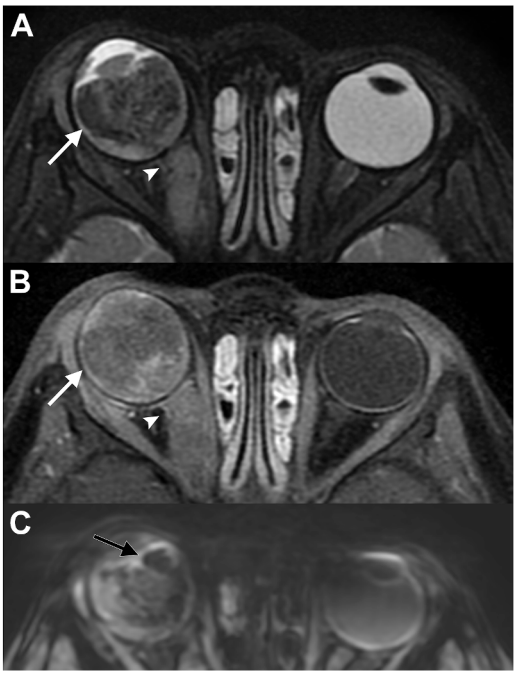

Fig. 14. Axial T2-weighted fat-suppressed (*A*) and fat-suppressed gadolinium-enhanced T1-weighted (*B*) and T2* (*C*) MR sequences show a right retinoblastoma with low T2-weighted signal and heterogeneous enhancement (*white arrows*). Blooming low signal on T2* (*black arrow*) indicates intralesional calcifications. There is optic nerve invasion (*white arrowhead*).

can show uveal thickening and enhancement, subretinal effusions (Fig. 12) and abnormal vitreous signal.

LEUKOCORIA AND INTRAOCULAR TUMORS

Leukocoria is loss of the normal red retinal reflex and signals an intraocular process that alters light reflection. It is non-specific and can result from a mass, membrane, retinal detachment or other retinal pathology; frequent causes include retinoblastoma, PFV, Coats' disease, ROP, among others.[17]

Retinoblastoma

Retinoblastoma is the most common primary intra-ocular tumor of childhood, diagnosed in about 80% of patients by age 3 years, and in 95% by age 5 years. It often arises from mutations in the RB1 tumor-suppressor gene.[18] The hereditary form can affect both eyes and predisposes survivors to later malignancies such as sarcomas, melanomas, and central nervous system tumors.[19] When bilateral ocular tumors are accompanied by a midline intracranial lesion in the suprasellar or pineal region the constellation is termed trilateral retinoblastoma (Fig. 13). Leptomeningeal spread can also occur.[18]

On CT, the presence of a hyperattenuating intraocular mass that demonstrates moderate contrast enhancement is characteristic. The presence of intraocular calcification in a child under the age of 3 years is highly suggestive of retinoblastoma.[20] On MR imaging, the lesion typically appears slightly hyperintense on T1-weighted images and hypointense on T2-weighted images relative to the surrounding vitreous. T2*-weighted images typically demonstrate low signal voids; linear peripheral areas of low signal may indicate hemorrhage while central nodular low signal suggests calcification (Fig. 14).[21] Following gadolinium administration, the lesion typically demonstrates heterogeneous enhancement.

Persistent Fetal Vasculature

PFV is a congenital failure of the embryonic hyaloid vascular system to regress normally and is the second most frequent cause of leukocoria after retinoblastoma.[20] It usually appears in full-term infants as unilateral leukocoria and microphthalmia,[17] although it may rarely be bilateral (Fig. 15). The hyaloid vascular system comprises

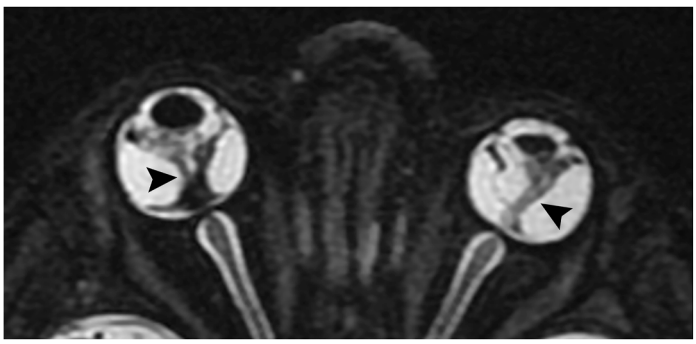

Fig. 15. Axial T2-weighted fat-suppressed MR imaging orbits demonstrating bilateral persistent fetal vasculature in a patient with Norrie's disease (*black arrowheads*).

Descargado para Lucia Angulo (lu.maru26@gmail.com) en National Library of Health and Social Security de ClinicalKey.es por Elsevier en julio 20, 2026.
Para uso personal exclusivamente. No se permiten otros usos sin autorización. Copyright ©2026. Elsevier Inc. Todos los derechos reservados.

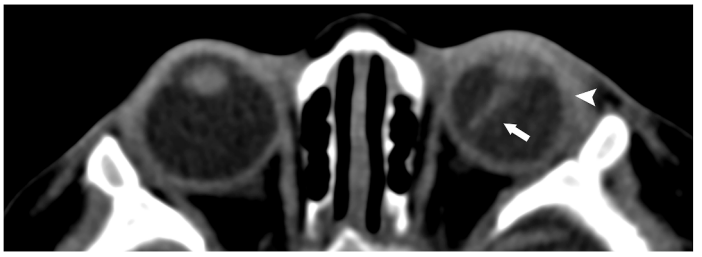

Fig. 16. Unenhanced axial CT orbits shows cone-shaped retrolental soft tissue along the expected Cloquet canal (*white arrow*) and mild left microphthalmia (*arrowhead*), findings consistent with persistent fetal vasculature.

an anastomotic vascular network arising from the hyaloid artery and supplies the developing lens, vitreous, and retina during embryogenesis. Fibrovascular adventitia and branches of the hyaloid artery extend from the retrolental region to the optic nerve head. It normally regresses leaving only the acellular Cloquet canal, which has a funnel-like configuration—narrow anteriorly near the optic nerve head and widening toward the lens. It is the incomplete involution of the hyaloid vascular network that results in PFV. On imaging, a fibrovascular stalk extends from a retrolental soft tissue to the posterior retina (**Fig. 16**), and traction on surrounding structures may cause retinal detachment, retinal or vitreous hemorrhage, and associated hypoplasia of the optic nerve.[22]

Coats Disease

Coats disease is a unilateral retinal vascular disorder with a strong male predilection, characterized by idiopathic retinal telangiectatic and aneurysmal vessels. These abnormal vessels lead to vascular leakage and progressive intraretinal and subretinal exudates, retinal thickening, and exudative retinal detachment. Advanced cases can mimic retinoblastoma.[23] Imaging usually shows retinal detachment without an intra-ocular mass, hyperintense subretinal exudates on both T1-weighted and T2-weighted MR imaging, and post-contrast enhancement of the detached retina, reflecting the underlying telangiectasia and microaneurysms (**Fig. 17**).[20]

Retinopathy of Prematurity

ROP is a bilateral vasoproliferative retinal disorder of premature infants, especially those with low birth weight and prolonged oxygen therapy or ventilatory support.[24] Normal retinal vascular development arrests and is followed by disorganized neovascularization. Although usually bilateral the disease can be asymmetrical. Early imaging findings are often nonspecific, with microphthalmia the most notable feature on CT or MR imaging.[1] Calcifications and retrolental soft tissue but may be seen in severe cases.[17] Diagnosis is primarily based on clinical history, including prematurity, incubator treatment, and ophthalmologic findings on ophthalmoscopy.[25]

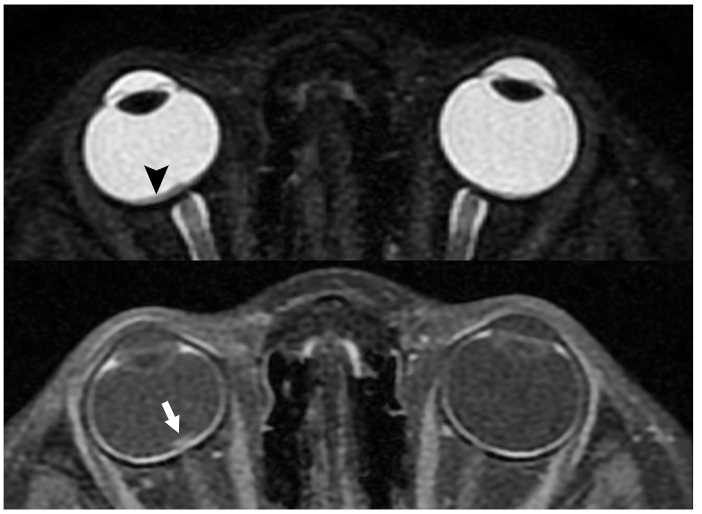

Fig. 17. Axial T2-weighted fat-suppressed and fat-suppressed gadolinium-enhanced T1-weighted MR sequences show small right subretinal exudates (*black arrowhead*), mild retinal enhancement (*white arrow*) and mild right microphthalmia. No enhancing mass is seen and findings are consistent with Coats disease.

Descargado para Lucia Angulo (lu.maru26@gmail.com) en National Library of Health and Social Security de ClinicalKey.es por Elsevier en julio 20, 2026. Para uso personal exclusivamente. No se permiten otros usos sin autorización. Copyright ©2026. Elsevier Inc. Todos los derechos reservados.

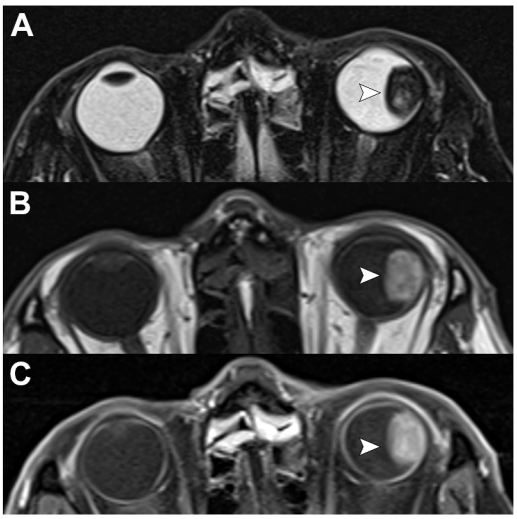

Fig. 18. Axial T2-weighted fat-suppressed (*A*), T1-weighted without fat-suppression (*B*) and fat-suppressed gadolinium-enhanced T1-weighted (*C*) MR sequences with a left T2-weighted hypointense, T1-weighted hyperintense, enhancing ovoid mass (*white arrowhead*). Histology confirmed uveal melanoma with abundant intracytoplasmic melanin pigment.

OTHER INTRAOCULAR TUMORS

Uveal Melanoma

Uveal melanoma is the most common primary intra-ocular tumor in adults, typically appearing in the 5th to 7th decade.[26] It most often arises in the choroid and may be asymptomatic or lead to reduced vision, floaters or field defects. Metastases spread chiefly to the liver, followed by the lung, bone and skin.[27]

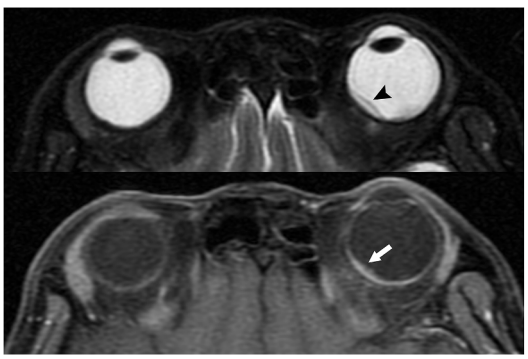

Fig. 19. Axial T2-weighted fat-suppressed (*top*) and fat-suppressed gadolinium-enhanced T1-weighted (*bottom*) MR sequences in a patient with breast cancer demonstrates a left choroid metastasis appearing as a curvilinear enhancing lesion at the posterior choroid (*white arrow*) with associated subretinal fluid (*arrowhead*).

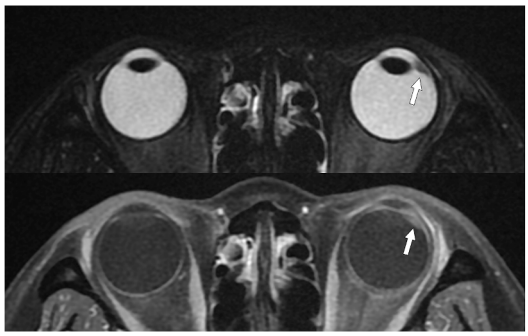

Fig. 20. Axial T2-weighted fat-suppressed (*top*) and fat-suppressed gadolinium-enhanced T1-weighted (*bottom*) MR sequences demonstrating a left ciliary body metastatic deposit on a background of breast carcinoma (*white arrows*).

Imaging appearances depend on melanin content. Melanotic tumors exhibit intrinsic T1-weighted and T2-weighted shortening: they are hyperintense on T1-weighted MR imaging, hypointense on T2-weighted images (**Fig. 18**), enhance post-contrast and often form mushroom-shaped peripheral masses with associated retinal or choroidal detachment.[28] Amelanotic melanomas lack significant melanin, appear hypointense on T1 and can resemble other intra-ocular neoplasms.[28,29] On CT, uveal melanomas present as hyperdense soft-tissue masses relative to vitreous and enhance post-contrast.

Uveal Metastasis

Uveal metastasis is the most common intra-ocular malignancy and a key differential when uveal melanoma is suspected. Unlike melanomas, which usually forms a protuberant, well-defined mass, metastatic lesions tend to spread along the choroid, giving a flatter mottled appearance with less thickening and less distinct margins (**Fig. 19**).[30] The commonest primary sources are breast and lung cancers (**Fig. 20**).[31]

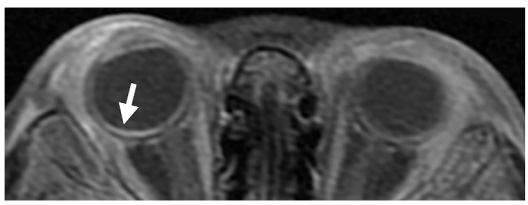

Fig. 21. Axial fat-suppressed gadolinium-enhanced T1-weighted sequence showing thin linear enhancement along the right posterior choroid, presumed diffuse choroidal hemangiomas with background Sturge-Weber syndrome (*white arrow*).

Descargado para Lucia Angulo (lu.maru26@gmail.com) en National Library of Health and Social Security de ClinicalKey.es por Elsevier en julio 20, 2026.
Para uso personal exclusivamente. No se permiten otros usos sin autorización. Copyright ©2026. Elsevier Inc. Todos los derechos reservados.

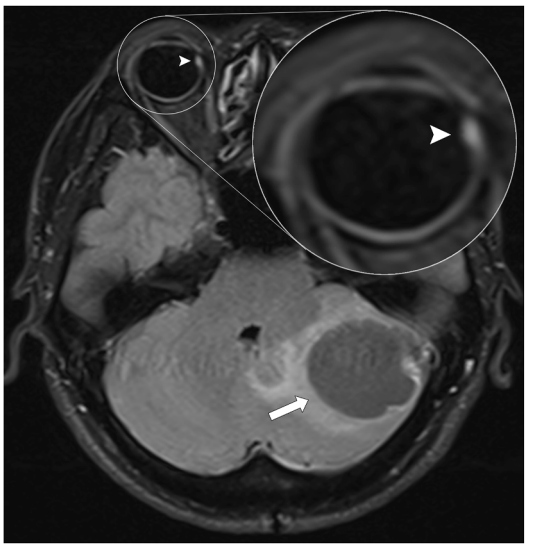

Fig. 22. Axial T2-weighted FLAIR and fat-suppressed sequence of the brain shows an enhancing focus at the medial right retina suggestive of a retinal angioma (*arrowheads* and figure inset). A left cerebellar hemangioblastoma (*arrow*) is also present in this patient with von Hippel–Lindau disease.

Imaging distinction from melanoma is difficult because signal characteristics often overlap. Metastases can also extend into the vitreous and cause retinal or choroidal detachment, mimicking melanoma.[31] T1-weighted MR imaging may separate metastasis from melanocytic tumors, but this becomes unreliable when hemorrhagic or mucinous material is present, as both can appear hyperintense.[29]

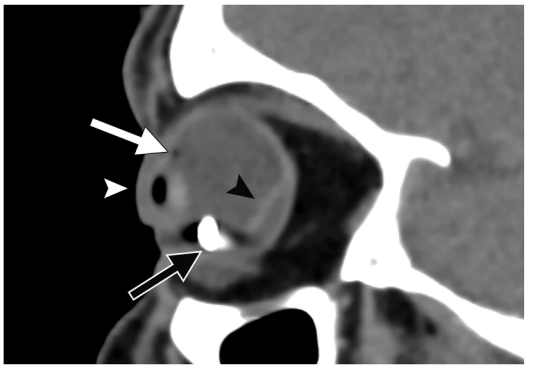

Fig. 23. Sagittal right CT orbit showing a hyperattenuating metallic intraocular foreign body (*black arrow*) with beam hardening artifacts. There is intraocular (*white arrow*) and anterior chamber gas (*white arrowhead*) and vitreous hemorrhage (*black arrowhead*). The globe shape appears preserved despite the penetrating foreign body.

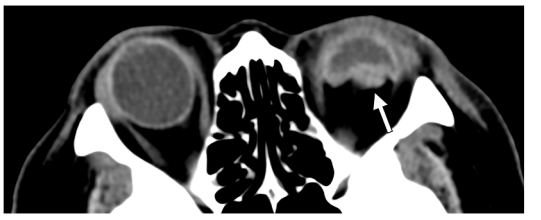

Fig. 24. Axial CT orbits showing a left globe rupture with crenated appearance (*white arrow*).

Choroidal and Retinal Vascular Lesions

Choroidal hemangiomas is a benign vascular tumor, typically seen in middle-aged to elderly individuals. It exists in 2 forms: a circumscribed (solitary) type, which occurs without systemic associations, and a diffuse form, commonly linked to Sturge-Weber syndrome.[31] On imaging, choroidal hemangiomas usually show T1-weighted hyperintensity, T2-weighted iso to hyperintensity and prominent post-contrast enhancement (**Fig. 21**).

Retinal angiomas, or retinal hemangioblastomas, are most often associated with von Hippel–Lindau disease (**Fig. 22**). They usually arise in the peripheral retina or at the juxtapapillary region and appear on ophthalmoscopy as round, pink-to-orange lesions with dilated tortuous feeder and draining vessels.[32] Complications include exudative retinal detachment, which can impair vision.[33]

OCULAR TRAUMA

As the most anterior part of the visual system, the globe is particularly susceptible to trauma. Injuries may be isolated or accompany facial trauma and are classified as blunt or penetrating injury.[34] Complications include open globe injury, lens dislocation, and intra-ocular hemorrhage.

Intraocular Foreign Body

Intraocular foreign bodies are a major concern in ocular trauma. CT is the preferred modality for

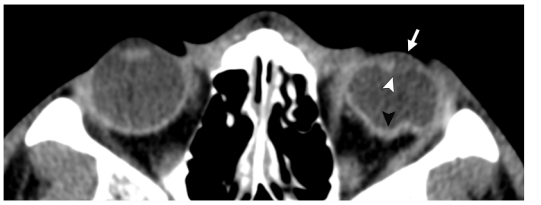

Fig. 25. Axial CT orbits of a patient with penetrating globe injury and corneal laceration showing abnormal hypodense appearance of the left lens (*white arrowhead*) and reduced volume of the anterior segment (*white arrow*). There is also left globe rupture (*black arrowhead*).

Descargado para Lucia Angulo (lu.maru26@gmail.com) en National Library of Health and Social Security de ClinicalKey.es por Elsevier en julio 20, 2026. Para uso personal exclusivamente. No se permiten otros usos sin autorización. Copyright ©2026. Elsevier Inc. Todos los derechos reservados.

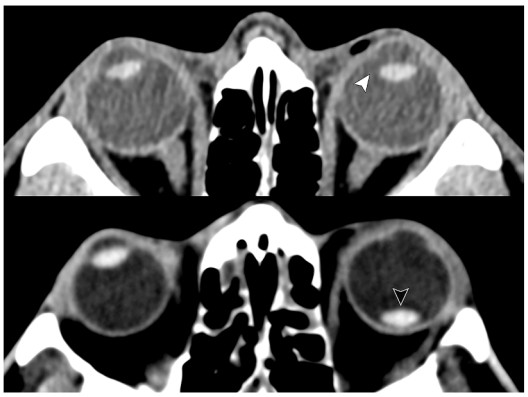

Fig. 26. Axial CT orbits demonstrating a left lens subluxation (*white arrowhead*) and posterior dislocation (*black arrowhead*).

detecting foreign bodies, especially metallic or paramagnetic ones which appear hyperdense on CT (**Fig. 23**), for which MR imaging is contraindicated.[35] Non-metallic foreign bodies can also be seen on CT, though MR imaging offers better soft-tissue contrast. Wood appears hypodense on CT,[36] similar to air, but as it absorbs moisture and becomes surrounded by granulation tissue, its attenuation increases to resemble fluid or soft tissue.[34] On MR imaging, non-metallic foreign bodies show uniformly low signal on T1, T2, and T2* sequences.

Globe Injury

Globe rupture may result from blunt or penetrating trauma. In blunt injury, rupture typically occurs at the globe's weakest points, especially just posterior to the extraocular muscle insertions where the sclera is thinnest.[35] Rupture may cause extrusion of intraocular contents, globe collapse and a crenated or wrinkled contour.[34]

CT is key in detecting open globe injuries. Findings include globe deformation or collapse (**Fig. 24**), intraocular air, foreign bodies, and hemorrhage in the aqueous or vitreous chambers. A full-thickness corneal laceration may allow aqueous humor to escape, reducing anterior chamber volume, and causing asymmetry (**Fig. 25**).[34] Posterior scleral rupture can lead to vitreous extrusion, lens retropulsion, and anterior segment enlargement.[37] Lens displacement, either anterior or posterior, may also be seen depending on the chamber affected. Crucially, some serious injuries may show no clear imaging signs, and a normal-appearing globe does not exclude an open globe injury (see **Fig. 23**).[38]

Table 2
Site of globe calcification and their common causes

Site of Calcification	Causes
Sclera	Senile calcific scleral plaques (**Fig. 28**) Hypercalcemia
Lens	Trauma
Uveal tract	Prior infection, for example, ocular toxoplasmosis (**Fig. 29**) Uveitis, choroiditis Sturge-Weber syndrome Choroidal osteoma
Retina	Retinoblastoma Drusen (**Fig. 30**) PFV, ROP, coats' disease Astrocytic hamartoma-associated with tuberous sclerosis (**Fig. 31**) Chronic organized retinal detachment

Traumatic Lens Injury

Globe trauma can disrupt the zonular fibers that anchor the lens, leading to subluxation or dislocation. Blunt trauma causes rapid globe deformation and zonular rupture,[1] while penetrating trauma may directly displace the lens into the vitreous. As the iris limits forward displacement, posterior dislocation into the vitreous is more common.[34]

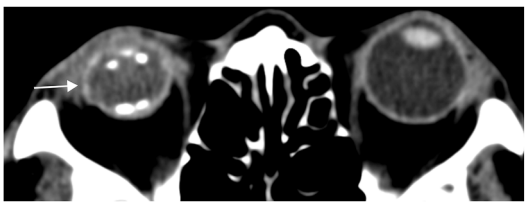

Fig. 27. Axial CT orbits demonstrating a shrunken and calcified right eye consistent with phthisis bulbi (*white arrow*).

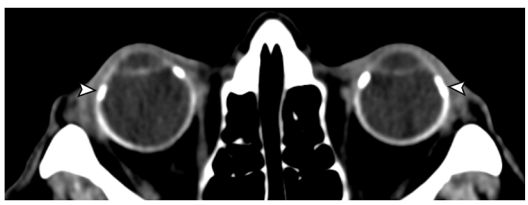

Fig. 28. Axial CT orbits demonstrating bilateral senile calcific scleral plaques with characteristic calcifications at the insertions of the medial and lateral recti muscles (*arrowheads*).

Descargado para Lucia Angulo (lu.maru26@gmail.com) en National Library of Health and Social Security de ClinicalKey.es por Elsevier en julio 20, 2026.
Para uso personal exclusivamente. No se permiten otros usos sin autorización. Copyright ©2026. Elsevier Inc. Todos los derechos reservados.

Fig. 29. Axial CT showing scleral calcifications in patient with prior right eye cytomegalovirus retinitis on a background of retroviral disease (*white arrow*).

Any abnormal lens position should raise suspicion for zonular injury.

On CT, the lens is normally hyperdense due to its high protein content. If the lens capsule is perforated, fluid can accumulate within the lens, resulting in opacification and a traumatic cataract, which appears hypodense (see **Fig. 25**).[39] While lens displacement is often clinically evident, imaging can confirm it, showing the lens either partially subluxed or lying dependently in the vitreous (**Fig. 26**).

INTRAOCULAR CALCIFICATIONS

Intraocular calcifications can be indicative of benign incidental findings to serious pathologies such as retinoblastoma. Some, like optic nerve head drusen or age-related sclerochoroidal calcifications, are often incidental and asymptomatic. Others may result from tumors (eg, retinoblastoma), chronic inflammation, or trauma. Recognizing the pattern, location, and associated imaging features can help avoid misdiagnosis and ensures appropriate ophthalmology referral.

Phthisis Bulbi

Phthisis bulbi refers to an end-stage, non-functional, atrophic eye, which is often partially calcified. It results from previous significant ocular injury, most commonly trauma or infection, and represents the final outcome of severe damage. Imaging shows a small, deformed, diminutive globe with curvilinear sclerochoroidal and dystrophic calcifications, particularly within the vitreous

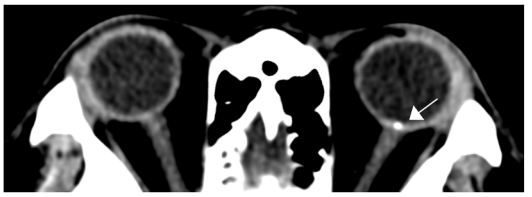

Fig. 30. Axial CT showing a calcified left optic nerve head drusen (*white arrow*).

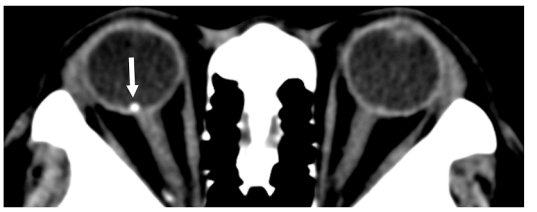

Fig. 31. Axial CT showing a calcified focus along the retina posteriorly consistent with a calcified astrocytic hamartoma in a patient with known tuberous sclerosis (*white arrow*).

humor (**Fig. 27**). Other common causes of intraocular calcifications are detailed in **Table 2**.[1,40,41]

OCULAR POSTSURGICAL CHANGES

Orbital imaging is often performed incidentally during brain, facial, or sinus studies, making radiologists commonly encounter postoperative ocular changes. Recognizing these findings is important, as they can mimic trauma, tumors, or inflammation. Common procedures include glaucoma drainage devices (GDDs), lens replacements, scleral buckling, silicone oil tamponade, pneumatic retinopexy, and globe prostheses.[35]

Glaucoma treatment aims to lower intraocular pressure using medical or surgical approaches. Surgery most often involves trabeculectomy or placement of GDDs. Trabeculectomy usually has no imaging findings on routine CT or MR imaging. A GDD has 2 components: a tube inserted into the anterior chamber, and a plate positioned in the superotemporal quadrant. On CT, the device appears as a curvilinear hyperdense structure adjacent to the globe. On MR imaging, it shows low signal on both T1-weighted and T2-weighted sequences. A small fluid-filled bleb may be seen

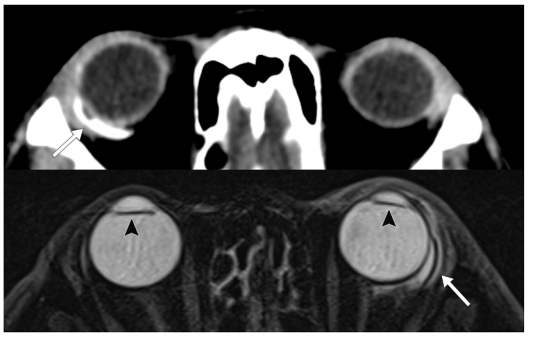

Fig. 32. Axial CT (*top*) and T2-weighted MR sequence (*bottom*) demonstrating glaucoma drainage devices on CT and MR respectively (*white arrows*), with small associated fluid filled blebs. Bilateral intraocular lens replacements also noted (*black arrowheads*).

Descargado para Lucia Angulo (lu.maru26@gmail.com) en National Library of Health and Social Security de ClinicalKey.es por Elsevier en julio 20, 2026. Para uso personal exclusivamente. No se permiten otros usos sin autorización. Copyright ©2026. Elsevier Inc. Todos los derechos reservados.

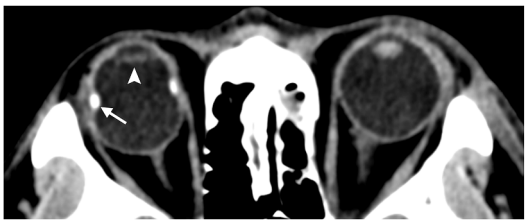

Fig. 33. Axial CT orbits showing a right scleral buckle (*arrow*) and intraocular lens replacement (*arrowhead*).

near the plate on MR imaging and can be mistaken for a cystic orbital lesion (**Fig. 32**).[42]

Cataract surgery typically involves using phacoemulsification to break up and remove the natural lens, followed by implantation of an artificial intraocular lens within the lens capsule. The artificial lens consists of 2 components: the optic and the footplates/haptics. The haptics are not readily visualized on imaging, whereas the artificial intraocular lens appears as a thin linear hyperdense structure posterior to the iris on CT and appears hypointense on MR imaging (**Fig. 33**).[42]

Surgical Treatment for Retinal Detachment

Ophthalmologists use several surgical techniques to repair retinal detachment, including scleral buckling, pars plana vitrectomy with intraocular tamponade, and retinopexy. The main goals are to re-appose the sensory retina with the RPE and to prevent the retinal tear from reopening.[43] Reattachment and sealing of the break are typically achieved through scleral buckling or tamponade.

Scleral buckling involves indenting the eye wall beneath the retinal break, reducing traction and promoting reattachment. On imaging, the buckle appears as an encircling band around the globe (see **Fig. 33**).

Vitrectomy entails removal of the vitreous gel, followed by insertion of a tamponade agent, either gas (eg, air or sulfur hexafluoride) or silicone oil, to close retinal breaks and re-appose the retina. On CT, intraocular gas appears as low attenuation within the vitreous cavity, often with air-fluid levels (**Fig. 34**); on MR imaging, it shows as hypointense on both T1-weighted and T2-weighted images.[42] Silicone oil appears hyperattenuating on CT (~130 HU), distinguishing it from blood (<90 HU).[44] On MR imaging, it typically shows T1 hyperintensity and variable T2 signal, often with chemical shift artifact at the oil–fluid interface (**Fig. 35**).

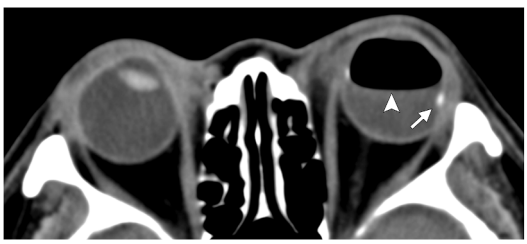

Fig. 34. Axial CT orbits showing a left pneumatic retinopexy with gas–fluid level (*arrowhead*) and a left scleral buckle (*arrow*).

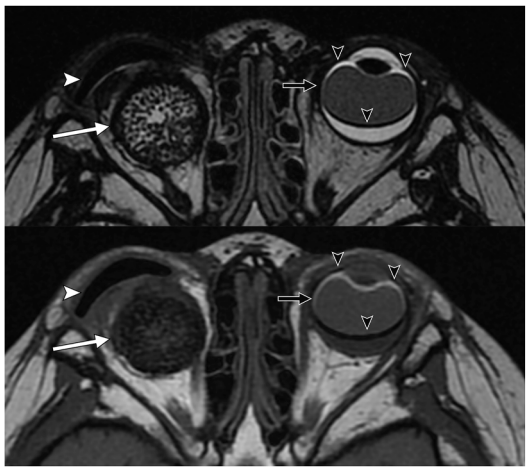

Fig. 35. Axial T2-weighted (*top*) and T1-weighted (*bottom*) MR sequences demonstrating a right porous orbital implant (*white arrow*) and ocular prosthesis (*white arrowhead*). Left intraocular silicone oil shows T2-weighted hypointense and T1-weighted hyperintense signal (*black arrows*). Note chemical shift artifacts at the oil–fluid interface (*black arrowheads*).

Orbital Implants

In severe ocular disease such as trauma, malignancy, or phthisis bulbi, enucleation may be required. After enucleation, a spherical orbital implant is placed to restore volume, followed by an ocular prosthesis resembling a large contact lens (**Fig. 36**). Implant materials include silicone, polymethylmethacrylate, and porous materials like porous polyethylene, which allow vascular ingrowth. On CT, porous polyethylene appears hypoattenuating with internal air foci (**Fig. 37**) that resolve as

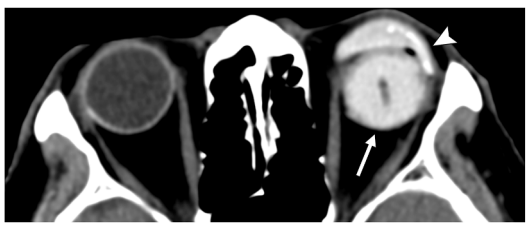

Fig. 36. Axial CT showing hyperdense left orbital implant (*arrow*) and ocular prosthesis (*arrowhead*).

Descargado para Lucia Angulo (lu.maru26@gmail.com) en National Library of Health and Social Security de ClinicalKey.es por Elsevier en julio 20, 2026.
Para uso personal exclusivamente. No se permiten otros usos sin autorización. Copyright ©2026. Elsevier Inc. Todos los derechos reservados.

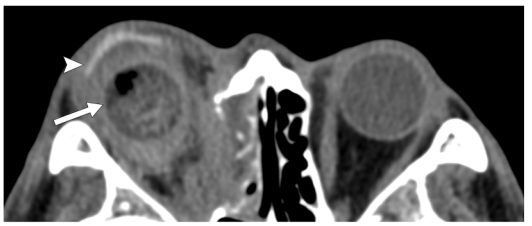

Fig. 37. Axial CT of a recent right porous polyethylene implant appearing hypodense with internal air foci (*white arrow*). Right ocular prosthesis (*arrowhead*).

fibrovascular tissue fills the implant.[42] Other porous implants may appear hyperdense on CT if made of calcium hydroxyapatite or aluminum oxide. On MR imaging, implants appear as hypointense globular structures on both T1-weighted and T2-weighted sequences (see **Fig. 35**).

SUMMARY

A wide range of globe abnormalities can be identified and evaluated using CT and MR imaging. Familiarity with CT attenuation patterns and MR imaging signal properties is essential for accurate lesion characterization. This article discusses the imaging features of various ocular pathologies as seen on CT and MR imaging.

CLINICS CARE POINTS

- A proficient understanding of the globe anatomy is essential for identifying the involved anatomical structure and its respective pathology.
- There are several intraocular potential spaces, each associated with specific types of ocular detachments that have characteristic imaging features.
- Leukocoria is a has a wide differential and imaging is helpful to between retinoblastoma and other mimics such as persistent fetal vasculature, Coats disease, and retinopathy of prematurity.
- Ocular trauma can cause specific injury patterns to the globe or lens with characterisitc imaging findings. Intraocular foreign bodies may be seen, often best seen on CT.
- Recognizing common postoperative ocular changes and implant devices is essential to avoid mistaking them for pathology and avoid unnecessary investigations.

DISCLOSURE

The authors have nothing to disclose.

REFERENCES

1. Cunnane ME, Sepahadari AR, Gardiner M, Mafee MF. Pathology of the eye and orbit. In: Som PM, Curtin HD, editors. Head and neck imaging. 5th edition. St Louis (MO): Elsevier Mosby; 2011. p. 591–649.
2. Kumar CM, Williamson S, Manickam B. A review of sub-Tenon's block: current practice and recent development. Eur J Anaesthesiol 2005;22(8):567–77.
3. Mafee MF, Karimi A, Shah J, et al. Anatomy and pathology of the eye: role of MR imaging and CT. Neuroimaging Clin 2005;15(1):23–47.
4. Forrester JV, Dick AD, McMenamin PG, et al. The eye: basic sciences in practice. 4th edition. London: Saunders/Elsevier; 2016.
5. Verma AS, FitzPatrick DR. Anophthalmia and microphthalmia. Orphanet J Rare Dis 2007;2(1):47.
6. Roos L, Jensen H, Grønskov K, et al. Congenital microphthalmia, anophthalmia and coloboma among live births in Denmark. Ophthalmic Epidemiol 2016; 23(5):324–30.
7. Ranga A, Yadav R, Bansal N, et al. Case series of intraorbital colobomatous cysts with anophthalmos/microphthalmos spectrum: a rare diagnostic conundrum simplified. Egypt J Radiol Nucl Med 2023; 54(1):172.
8. Grech R, Spiteri Cornish K, Galvin PL, et al. Imaging of adult ocular and orbital pathology - a pictorial review. Radiology Case 2014;8(2):1–29.
9. McNicholas MM, Brophy DP, Power WJ, et al. Ocular sonography. Am J Roentgenol 1994;163(4): 921–6.
10. LeBedis CA, Sakai O. Nontraumatic orbital conditions: diagnosis with CT and MR imaging in the emergent setting. Radiographics 2008;28(6):1741–53.
11. Mafee MF, Linder B, Peyman GA, et al. Choroidal hematoma and effusion: evaluation with MR imaging. Radiology 1988;168(3):781–6.
12. Hallinan JT, Pillay P, Koh LH, et al. Eye Globe Abnormalities on MR and CT in adults: an anatomical approach. Korean J Radiol 2016;17(5):664–73.
13. Ferreira TA, Saraiva P, Genders SW, et al. CT and MR imaging of orbital inflammation. Neuroradiology 2018;60(12):1253–66.
14. Diogo MC, Jager MJ, Ferreira TA. CT and MR imaging in the diagnosis of scleritis. AJNR Am J Neuroradiol 2016;37(12):2334–9.
15. Osman Saatci A, Saatci I, Kocak N, et al. Magnetic resonance imaging characteristics of posterior scleritis mimicking choroidal mass. Eur J Radiol 2001;39(2):88–91.
16. Li CQ, Cho AA, Edward NJ, et al. Magnetic resonance imaging of uveitis. Neuroradiology 2015; 57(8):825–32.
17. Kadom N, Sze RW. Radiological reasoning: leukocoria in a child. Am J Roentgenol 2008;191(3_supplement): S40–4.

Descargado para Lucia Angulo (lu.maru26@gmail.com) en National Library of Health and Social Security de ClinicalKey.es por Elsevier en julio 20, 2026. Para uso personal exclusivamente. No se permiten otros usos sin autorización. Copyright ©2026. Elsevier Inc. Todos los derechos reservados.

18. Rauschecker AM, Patel CV, Yeom KW, et al. High-Resolution MR imaging of the orbit in patients with retinoblastoma. Radiographics 2012;32(5):1307–26.
19. Wong JR, Morton LM, Tucker MA, et al. Risk of subsequent malignant neoplasms in long-term hereditary retinoblastoma survivors after chemotherapy and radiotherapy. J Clin Orthod 2014;32(29):3284–90.
20. Apushkin MA, Apushkin MA, Shapiro MJ, et al. Retinoblastoma and simulating lesions: role of imaging. Neuroimaging Clin 2005;15(1):49–67.
21. Pai V, Muthusami P, Ertl-Wagner B, et al. Diagnostic imaging for retinoblastoma cancer staging: guide for providing essential insights for ophthalmologists and oncologists. Radiographics 2024;44(4):e230125. https://doi.org/10.1148/rg.230125.
22. Chen C, Xiao H, Ding X. Persistent fetal vasculature. Asia-Pacific. J Ophthalmol 2019;8(1):86–95.
23. Jansen RW, De Bloeme CM, Brisse HJ, et al. MR imaging features to differentiate retinoblastoma from coats' disease and persistent fetal vasculature. Cancers 2020;12(12):3592.
24. Hopper KD, Sherman JL, Boal DK. Abnormalities of the orbit and its contents in children: CT and MR imaging findings. Am J Roentgenol 1991;156(6):1219–24.
25. Valikodath N, Cole E, Chiang MF, et al. Imaging in retinopathy of prematurity. Asia Pac J Ophthalmol (Phila) 2019;8(2):178–86.
26. Jager MJ, Shields CL, Cebulla CM, et al. Uveal melanoma. Nat Rev Dis Primers 2020;6(1):24.
27. Woodman SE. Metastatic uveal melanoma: biology and emerging treatments. Cancer J 2012;18(2):148–52.
28. Wong VK, Lubner MG, Menias CO, et al. Clinical and imaging features of noncutaneous melanoma. Am J Roentgenol 2017;208(5):942–59.
29. Peyster RG, Augsburger JJ, Shields JA, et al. Intraocular tumors: evaluation with MR imaging. Radiology 1988;168(3):773–9.
30. Konstantinidis L, Damato B. Intraocular metastases–a review. Asia Pac J Ophthalmol (Phila) 2017;6(2):208–14.
31. Mafee MF. Uveal melanoma, choroidal hemangioma, and simulating lesions. Role of MR imaging. Radiol Clin North Am 1998;36(6):1083–x.
32. Singh AD, Shields CL, Shields JA. von Hippel-Lindau disease. Surv Ophthalmol 2001;46(2):117–42.
33. Webster AR, Maher ER, Moore AT. Clinical characteristics of ocular angiomatosis in von hippel-lindau disease and correlation with germline mutation. Arch Ophthalmol 1999;117(3):371.
34. Balakrishnan S, Harsini S, Reddy S, et al. Imaging review of ocular and optic nerve trauma. Emerg Radiol 2020;27(1):75–85.
35. Roy AA, Davagnanam I, Evanson J. Abnormalities of the globe. Clin Radiol 2012;67(10):1011–22.
36. Specht CS, Varga JH, Jalali MM, et al. Orbitocranial wooden foreign body diagnosed by magnetic resonance imaging. Dry wood can be isodense with air and orbital fat by computed tomography. Surv Ophthalmol 1992;36(5):341–4.
37. Yuan WH, Hsu HC, Cheng HC, et al. CT of globe rupture: analysis and frequency of findings. Am J Roentgenol 2014;202(5):1100–7.
38. Joseph DP, Pieramici DJ, Beauchamp NJ. Computed tomography in the diagnosis and prognosis of open-globe injuries. Ophthalmology 2000;107(10):1899–906.
39. Segev Y, Goldstein M, Lazar M, et al. CT appearance of a traumatic cataract. AJNR Am J Neuroradiol 1995;16(5):1174–5.
40. Zeiter HJ. Calcification and ossification in ocular tissue. Am J Ophthalmol 1962;53(2):265–74.
41. Hedges TR, Pozzi-Mucelli R, Char DH, et al. Computed tomographic demonstration of ocular calcification: Correlations with clinical and pathological findings. Neuroradiology 1982;23(1):15–21.
42. Reiter MJ, Schwope RB, Kini JA, et al. Postoperative imaging of the orbital contents. Radiographics 2015;35(1):221–34.
43. Lane JI, Watson RE, Witte RJ, et al. Retinal detachment: imaging of surgical treatments and complications. Radiographics 2003;23(4):983–94.
44. Mathews VP, Elster AD, Barker PB, et al. Intraocular silicone oil: in vitro and in vivo MR and CT characteristics. AJNR Am J Neuroradiol 1994;15(2):343–7.

Descargado para Lucia Angulo (lu.maru26@gmail.com) en National Library of Health and Social Security de ClinicalKey.es por Elsevier en julio 20, 2026.
Para uso personal exclusivamente. No se permiten otros usos sin autorización. Copyright ©2026. Elsevier Inc. Todos los derechos reservados.